

Geophysical Research Letters®



RESEARCH LETTER

10.1029/2024GL108194

Physical and Biogeochemical Phenology of Coastal Upwelling in the California Current System

Ellen M. Jorgensen^{1,2} , Elliott L. Hazen^{3,4} , Michael G. Jacox^{3,4,5} , Mercedes Pozo Buil^{3,4} , Isaac Schroeder^{3,4}, and Steven J. Bograd^{3,6} 

¹Department of Earth and Environmental Sciences, Syracuse University, Syracuse, NY, USA, ²Department of Earth, Environmental & Planetary Sciences, Brown University, Providence, RI, USA, ³NOAA Southwest Fisheries Science Center, Monterey, CA, USA, ⁴Institute of Marine Sciences, University of California-Santa Cruz, Santa Cruz, CA, USA, ⁵NOAA Physical Sciences Laboratory, Boulder, CO, USA, ⁶Department of Ocean Sciences, University of California-Santa Cruz, Santa Cruz, CA, USA

Key Points:

- We define new upwelling phenology indices for the California Current System that include nutrient transport
- We identify spatial, seasonal, and interannual patterns of upwelling and nutrient delivery
- We relate the physical mechanisms of coastal upwelling with its biological efficacy

Supporting Information:

Supporting Information may be found in the online version of this article.

Correspondence to:

E. M. Jorgensen,
ellen_jorgensen@brown.edu

Citation:

Jorgensen, E. M., Hazen, E. L., Jacox, M. G., Pozo Buil, M., Schroeder, I., & Bograd, S. J. (2024). Physical and biogeochemical phenology of coastal upwelling in the California Current System. *Geophysical Research Letters*, 51, e2024GL108194. <https://doi.org/10.1029/2024GL108194>

Received 8 JAN 2024
Accepted 21 MAR 2024

Author Contributions:

Conceptualization: Elliott L. Hazen, Michael G. Jacox, Steven J. Bograd
Data curation: Ellen M. Jorgensen, Michael G. Jacox, Isaac Schroeder
Formal analysis: Ellen M. Jorgensen, Michael G. Jacox
Supervision: Michael G. Jacox, Isaac Schroeder, Steven J. Bograd
Writing – original draft: Ellen M. Jorgensen, Steven J. Bograd
Writing – review & editing: Ellen M. Jorgensen, Elliott L. Hazen, Michael G. Jacox, Mercedes Pozo Buil, Isaac Schroeder, Steven J. Bograd

Abstract In the California Current System (CCS), changes in the phenology (i.e., seasonal timing) of coastal upwelling alter the functioning of this productive marine ecosystem. Recently developed coastal upwelling indices that account for upwelling strength and nutrient flux to the surface provide a more complete understanding of bottom-up forcing in the region. Using these indices, we describe CCS upwelling phenological variability in vertical transport and nutrient flux. Physical and biogeochemical spring transitions generally occur in winter or spring, followed by increased upwelling and nutrient flux. In the latter half of the year, upwelling continues but nutrient flux wanes as declining source nutrient concentrations limit the biological efficacy of coastal upwelling. Earlier spring transitions and higher season-integrated upwelling intensity occur during strong La Niña events at all latitudes, driven largely by stronger alongshore wind stress. Understanding phenological changes in coastal upwelling is critical, as they could have significant ecosystem consequences.

Plain Language Summary In the California Current System (CCS), coastal upwelling carries nutrient-rich waters to the surface, supporting primary production and driving the coastal ecosystem. This upwelling varies on a seasonal and interannual basis, as reflected in recently developed indices that account for the amount of water upwelled to the surface as well as the amount of nutrients carried in that water. Generally upwelling and nutrient transport are high in the first half of the year. Upwelling persists into the second half of the year, but nutrient transport decreases as the deep-water sources of these nutrients are depleted. Upwelling in the CCS is also affected by the El Niño Southern Oscillation. During La Niña conditions, strong trade winds enhance upwelling and nutrient transport on the California coast. This paper presents regional, seasonal and interannual patterns of upwelling and nutrient delivery in the CCS, which are important drivers of change to this coastal ecosystem.

1. Introduction

In the California Current System (CCS), wind-driven coastal upwelling draws nutrient-rich water from depth and fuels rich and diverse biological populations at all trophic levels. The amount of nutrients delivered to the euphotic zone depends both on the total volume of upwelled water and on the nutrient content of that water, which are controlled by a complex interaction of physical processes including the strength and spatial variability of equatorward wind stress, near-surface ocean circulation, the vertical structure of the water column and the supply of available nutrients at the upwelling source depth (Bograd et al., 2023; Jacox et al., 2015). Each of these physical processes determine the efficacy of coastal upwelling and can vary independently across spatial and temporal scales. In fact, nonlinear interactions between the influences of winds and nutrient content result in spatially varying optimal environmental conditions that drive phytoplankton biomass (Jacox et al., 2016).

The *phenology*, or seasonal timing, of coastal upwelling strongly influences the distribution of nutrients available to fuel primary production and in turn trophic interactions in coastal marine ecosystems (Cushing, 1990; Durant et al., 2007). Bograd et al. (2009) developed indices to define the phenological patterns of coastal upwelling in the CCS. These indices include the *Spring Transition Index (STI)*, the date of minimum cumulative upwelling integrated from the beginning of the calendar year; *Length of Upwelling Season Index (LUSI)*, the number of days between the dates of minimum and maximum cumulative upwelling; and *Total Upwelling Magnitude Index (TUMI)*, the integrated magnitude of upwelling between the start and end of the upwelling season. These indices

© 2024. The Authors.

This is an open access article under the terms of the [Creative Commons Attribution License](https://creativecommons.org/licenses/by/4.0/), which permits use, distribution and reproduction in any medium, provided the original work is properly cited.

were derived from the classical Bakun upwelling index, which uses coarsely resolved sea level pressure fields and Ekman theory to derive estimates of offshore Ekman transport as a proxy for coastal upwelling (Bakun, 1973, 1975; Schwing et al., 1996). The simplicity of the Bakun index, as well as its continuity over several decades, have made it a keystone metric for investigating the effects of upwelling on coastal marine ecosystems in many regions and across trophic levels (e.g., Asch, 2015; Botsford et al., 2006; Garcia-Reyes et al., 2014; Lamont et al., 2018). The simplicity of the Bakun index, however, limits its capacity to accurately represent the coastal upwelling process due to uncertainties in the estimation of wind stress, omission of the influences of ocean circulation, and a lack of information on the nutrient content of upwelled waters.

Jacox et al. (2018) derived new coastal upwelling indices for the CCS that address these limitations by leveraging advances in regional ocean models. These new indices provide improved estimates of vertical transport as well as estimates of the vertical nitrate flux, and hence the potential biological utility of coastal upwelling. In this study, we develop and evaluate new phenological indices for the CCS derived from the new coastal upwelling indices to discern both the physical and biogeochemical drivers of upwelling seasonality along the U.S. West Coast. Our analysis provides an improved and updated investigation of regional and interannual variability in upwelling phenology in the CCS.

2. Data and Methods

2.1. CUTI and BEUTI

We derived annual phenological indices from recently developed California Current upwelling indices that were developed to improve the representation of the wind-driven transport, account for the influence of geostrophic currents, and estimate vertical nitrate flux. These indices are described in detail by Jacox et al. (2018); here we introduce them briefly. The Coastal Upwelling Transport Index (CUTI) quantifies vertical transport, estimated as the sum of the near-surface Ekman transport (driven by alongshore winds and wind stress curl) and cross-shore geostrophic flow (driven by the alongshore pressure gradient). CUTI is an improved version of the classical Bakun upwelling index (Bakun, 1973, 1975; Schwing et al., 1996), with improved resolution of surface winds and inclusion of the geostrophic component that often counteracts Ekman transport and reduces the magnitude of vertical transport (Colas et al., 2008; Jacox et al., 2018; Marchesiello & Estrade, 2010). The Biologically Effective Upwelling Transport Index (BEUTI) provides an estimate of vertical nitrate flux in coastal waters, and thus is more directly related to upwelling-induced biological production. BEUTI is calculated as the product of the vertical transport at the base of the mixed layer (i.e., CUTI) and the nitrate concentration at the base of the mixed layer, with the latter estimated from an observationally derived temperature-latitude-nitrate relationship (Jacox et al., 2018). Mixed layer depth (MLD) was calculated using a density change associated with a 0.8°C temperature change relative to a 10 m reference depth, following Kara et al. (2000). For both CUTI and BEUTI, oceanographic conditions and surface wind stresses are obtained from the output of data assimilative regional ocean models for the CCS (Neveu et al., 2016; oceanmodeling.ucsc.edu). CUTI and BEUTI are calculated at daily resolution over the period 1988–2022, with each index computed for bins of 1° latitude along the U.S. West Coast from 31°N to 47°N and extending 75 km offshore.

2.2. Phenological Indices

Following the methodology of previously derived phenological indices (Bograd et al., 2009), we first consider the cumulative CUTI and BEUTI (i.e., the sum of daily values beginning January 1st) at each location for each calendar year. The beginning of the upwelling season, defined as the STI, is calculated as the date of minimum cumulative upwelling in the first half of the year (i.e., the date at which vertical transport shifts from predominantly downwelling to predominantly upwelling). Similarly, the end of the upwelling season is the date of maximum cumulative upwelling in the second half of the year, and the number of days between the start and end of the upwelling season is defined as the length of the upwelling season (LUSI). The TUMI is the integrated daily upwelling index between the start and end of the upwelling season. Total Upwelling Magnitude Index, which has different units in CUTI and BEUTI, respectively, was standardized by subtracting the mean and dividing by the standard deviation. Each phenological index (STI, LUSI, TUMI) is derived separately for CUTI and BEUTI, anomalies are calculated from the 35-year means, and all indices are compared amongst CUTI, BEUTI and Bakun.

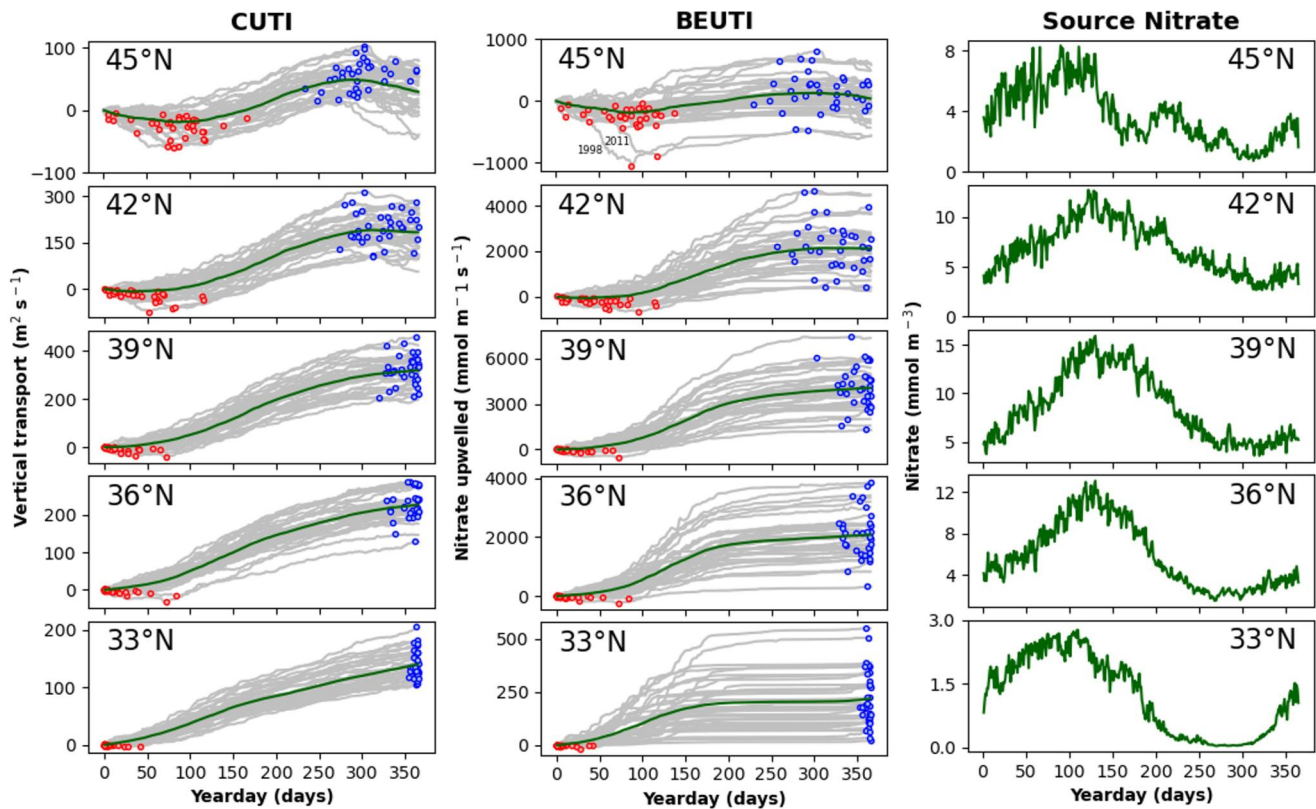


Figure 1. Cumulative daily Coastal Upwelling Transport Index ($\text{m}^2 \text{s}^{-1}$; left panels) and Biologically Effective Upwelling Transport Index ($\text{mmol m}^{-1} \text{s}^{-1}$; center panels) at 33°N , 36°N , 39°N , 42°N , and 45°N for all years (1988–2022; gray curves) and for the 33-year mean (green curves); mean daily nitrate flux at base of mixing layer from 1988–2022 mmol L^{-1} ; right panels; note scale difference on y-axes). Spring transition (date of minimum cumulative upwelling) is marked in red for each year; end of upwelling season (date of maximum cumulative upwelling) is marked in blue for each year.

3. Results

3.1. Physical and Biogeochemical Phenological Indices

We show here results in three latitudinal locations across the CCS: 33°N , 39°N , and 45°N , representative of southern, central, and northern regions, respectively. The annual cycle of cumulative CUTI shows strongest upwelling magnitude at 39°N , pronounced winter downwelling at 45°N and persistent year-round upwelling, though relatively weak, at 33°N (Figure 1). The climatological spring transition occurs earlier at southern latitudes (day 0 at 39°N , day 84 at 45°N), which also have a longer upwelling season (LUSI) in the mean. These broad coastwide patterns are similar to those of the phenological indices derived from the classical Bakun upwelling index (Bograd et al., 2009).

The annual cycle of cumulative BEUTI shows different patterns compared to those of CUTI (Figure 1). Discrepancies between CUTI and BEUTI can be attributed to changes in subsurface nitrate availability as BEUTI is the product of CUTI and the concentration of nitrate at the base of the mixed layer. Across all latitudes, we see a plateau of cumulative BEUTI in the second half of the year, which reflects limited availability of nitrate going into the fall and winter seasons (Figure 1). We see the highest upwelled nitrate at 39°N , driven by the stronger winds along the central and northern California coast, with the cumulative BEUTI plateau occurring around Julian day 250 (September). Both the lower and higher latitudes have an earlier plateau in cumulative BEUTI (around Julian day 175, June), with a mean negative nitrate flux during the winter downwelling season at 45°N . In fact, the mean cumulative BEUTI in the northern CCS is nearly flat through the year, but there were 2 years (1998, 2011) with anomalously negative nitrate flux in the first half of the year. There is substantial interannual variability in nitrate availability at 33°N , with some years having almost no nitrate flux at all, likely a result of low source nitrate (note low nitrate availability at 33°N in Figure 1) and weak winds.

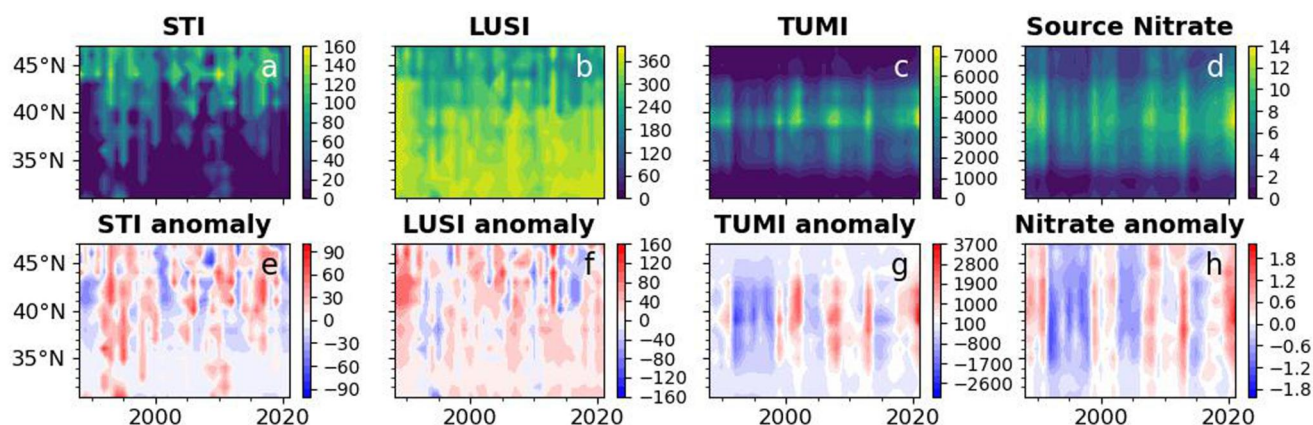


Figure 2. Hovmöller diagrams of phenological indices derived from Biologically Effective Upwelling Transport Index (a–c, e–g) and mean annual source nitrate concentration (d, h). First column panels are the spring transition index (STI; yearday) and STI anomaly (days) from the 35-year mean. Second column panels are the length of upwelling index (LUSI; days) and Length of Upwelling Season Index anomaly (days) from the 35-year mean. Third column panels are the total upwelling magnitude index (TUMI; $\text{mmol m}^{-2} \text{s}^{-1}$) and TUMI anomaly ($\text{mmol m}^{-2} \text{s}^{-1}$) from the 35-year mean. Fourth column panels are the mean annual nitrate concentration at the base of the mixing layer (mmol L^{-1}) and annual nitrate concentration anomaly ($\mu\text{mol L}^{-1}$) from the 35 years mean.

3.2. Regional and Interannual Variability

Hovmöller diagrams of the CUTI and BEUTI phenological indices demonstrate their meridional and interannual variability, as well as the relative contributions of wind forcing and nitrate variability to the seasonal nitrate fluxes (Figure 2). STI and LUSI show similar patterns of variability for CUTI and BEUTI, with years of anomalously early or late spring transition (and end of upwelling season) generally occurring coastwide. Despite the differences in seasonally- and latitudinally varying nitrate availability, the duration of the physical upwelling season and the “biologically effective” upwelling season are similar. More significant differences are evident between the upwelling-season integrated CUTI and BEUTI (i.e., TUMI; Figure 2). The relatively lower values of BEUTI-derived TUMI at the lower latitudes shows that, though weak upwelling occurs year-round here, there is less available nitrate at depth. In general, a decoupling of CUTI and BEUTI, and their derived phenological indices, can occur when the seasonality of winds and nitrate supply are out of phase, for example, in the northern CCS in winter when upwelling is weak while subsurface nitrate is high due to deep mixing (Figure 4). More broadly, BEUTI is driven more by nitrate supply than CUTI in the central CCS but more by CUTI in the northern CCS (Jacox et al., 2018; Figure 11) during the upwelling season, reflecting the observation that the southern CCS is more strongly influenced by remote forcing that modulates nitrate fluxes through water column changes while the northern CCS is influenced more by local wind forcing that alters nitrate flux through changes in upwelling/downwelling (Frischknecht et al., 2015). Comparing CUTI and BEUTI across the CCS during El Niño and La Niña conditions allows us to highlight the variability of productivity between these climate states (Figure 3). El Niño BEUTI falls significantly lower than that of La Niña states, particularly in the southern CCS. The phenological indices of CUTI and BEUTI also reveal extended periods of anomalously low vertical nitrate flux coastwide during the 1990s, and shorter periods of anomalously high vertical nitrate flux from 2002 to 2007 and post-2017. These periods of higher and lower nutrient input appear to mostly be driven by anomalous wind forcing (Figure 2).

3.3. Comparisons With Bakun Upwelling Index

Phenological indices derived from CUTI and BEUTI can differ up to 20% from those derived from the traditional Bakun upwelling index (Figure S1). While the CUTI- and BEUTI-derived spring transition dates are comparable in the northern, central and southern CCS, they generally occur earlier in the year than those derived from the Bakun upwelling index, resulting in longer estimates of upwelling season duration. Late Bakun-derived spring transitions are especially frequent in the southern CCS and are often in large contrast to those derived from CUTI and BEUTI, indicating the importance of improved estimates of wind and geostrophic flow used in CUTI. The divergence of the Bakun Index phenology from observations, especially off California, was noted at the outset by Bakun (1973, 1975). For example, he found from wind observations that offshore Ekman transport occurred year-round as far north as $\sim 40^\circ\text{N}$, while his SLP-based upwelling index showed seasonal downwelling as far south as

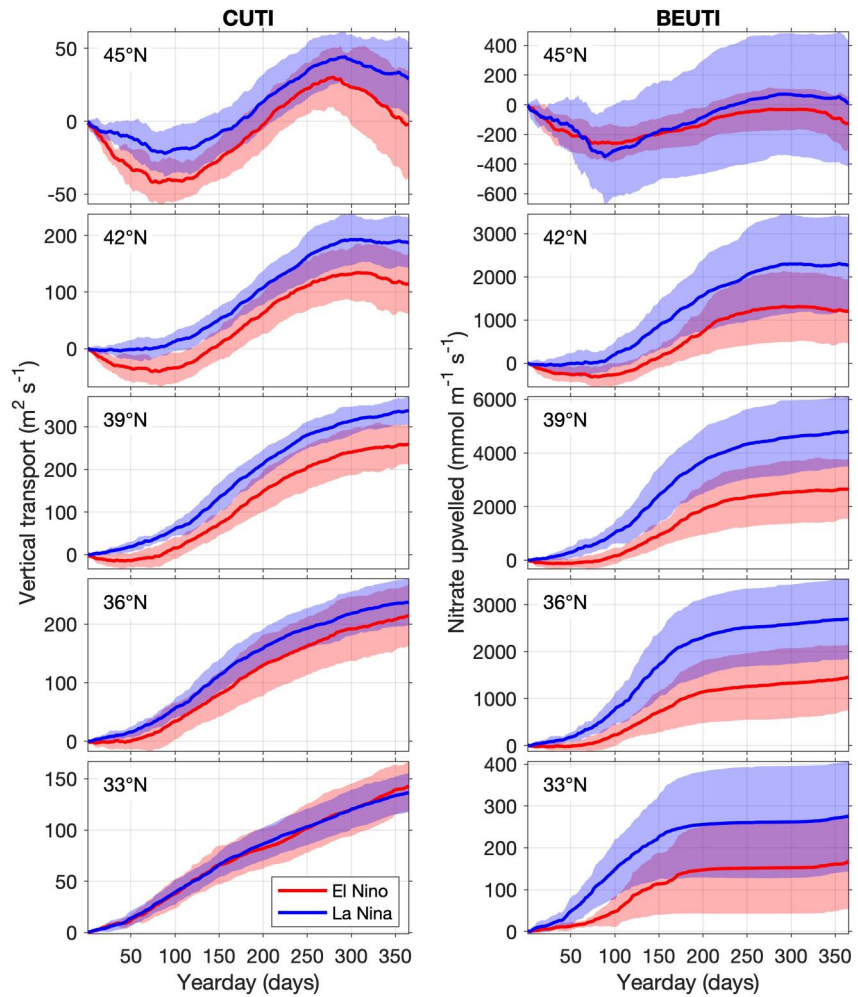


Figure 3. Cumulative daily Coastal Upwelling Transport Index ($\text{m}^2 \text{s}^{-1}$; left panels) and Biologically Effective Upwelling Transport Index ($\text{mmol m}^{-1} \text{s}^{-1}$; right panels) at 45°N , 42°N , 39°N , 36°N , and 33°N for composites of years following the peak of moderate to strong El Niño events (red; 1992, 1995, 1998, 2003, 2010, 2016) and La Niña events (blue; 1989, 1996, 1999, 2000, 2008, 2011, 2012, 2021, 2022). Solid lines represent the mean across years while shading indicates ± 1 standard deviation.

$\sim 35^\circ\text{N}$ (see Figure 3 in Jacox et al., 2018). A similar effect is seen for the fall transition (earlier in the Bakun Index than in wind observation-based estimates). Because the cumulative BEUTI tends to asymptote in late summer, the date marking the end of the upwelling season, and hence LUSI, may not always reflect the end of significant change to upwelling. For example, based on the annual maximum of cumulative BEUTI, the end of the upwelling season is recorded in the last few days of the year for all results from 1988 to 2022 (Figure 1). If we instead defined the end of the upwelling season as the date at which cumulative BEUTI reaches 90% of its annual maximum, there is often a much earlier end to the upwelling season (yearday 150–200), and thus a shorter upwelling season, especially in the central and southern CCS.

Standardized TUMI differs amongst the three indices, although they all show similar low-frequency variability, especially in the central CCS where upwelling is strongest (Figure S1). Bakun-derived TUMI is driven largely by upwelling season duration ($r^2 = 0.91$ for $\text{LUSI}_{\text{Bakun}}$ vs. $\text{TUMI}_{\text{Bakun}}$ at 39°N). The differences in CUTI- and BEUTI-derived TUMI, however, are attributable to regional and interannual variations in nitrate supply. For example, the contrasting high (BEUTI) versus low (CUTI) TUMI values at 45°N in 2009 suggests an anomalously high nitrate supply in the northern CCS that year (see Figure S1 from Jacox et al., 2015 for modeled nitrate supply).

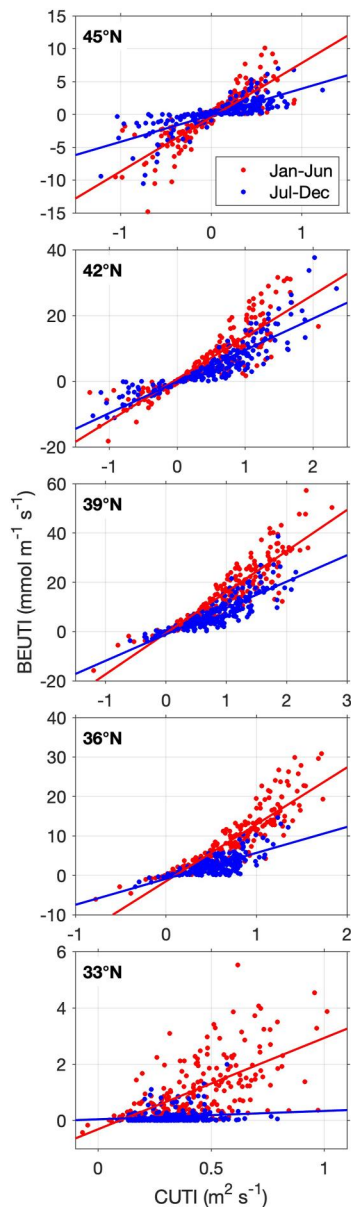


Figure 4. Coastal Upwelling Transport Index (CUTI) ($\text{m}^2 \text{s}^{-1}$; x-axis) versus Biologically Effective Upwelling Transport Index (BEUTI) ($\mu\text{mol m}^{-1} \text{s}^{-1}$; y-axis) shown for all years (1988–2022) at 45°N, 42°N, 39°N, 36°N, and 33°N for the first (red dots) and second (blue dots) half of the year. Linear regressions for each half of the year (red and blue lines) demonstrate seasonal decoupling of CUTI and BEUTI.

the North Pacific High is expected to lead to stronger alongshore winds in the northern CCS and a weakening of upwelling intensity in the southern CCS (Bograd et al., 2023; Rykaczewski et al., 2015). The increase in upwelling intensity in the central and northern CCS is particularly evident in April–May, leading to an earlier spring transition and potentially a longer upwelling season (Rykaczewski et al., 2015). While these models provide relatively robust projections of the magnitude and timing of CUTI, an ensemble of regional downscaled climate models for the CCS quantifies projected changes in water column structure and nutrient content (Pozo Buil et al., 2021). In these models, the MLD is projected to shoal system wide with different responses in the subsurface nitrate concentration, which can lead to an overall weak negative trend (central CCS) to no trend (southern and northern CCS) in BEUTI (Bograd et al., 2023; Pozo Buil et al., 2021). These patterns generally suggest a decline in primary productivity in the CCS, although there is significant variability in those projections (Bograd

4. Conclusions

Here we quantify regional and interannual variability in the phenology of coastal upwelling in the CCS using new, more accurate upwelling indices that leverage state-of-the-art ocean models, satellite data and in situ observations. The physical and biogeochemical spring transition are generally coincident and occur earlier than estimates derived from the classical Bakun upwelling index. The duration of the physical and biogeochemical upwelling season differs, however, and is sensitive to the definition of the fall transition (Figure S1). Nitrate concentration at the base of the mixed layer peaks in spring when upwelling intensity (CUTI) is highest and subsequently decreases through the summer upwelling season to a fall minimum (Jacox et al., 2018; Figure S1). Even as cumulative CUTI increases until there is a reduction or reversal in the equatorward alongshore winds in fall (in the central and northern CCS), cumulative BEUTI approaches its annual maximum in mid to late summer as stratification increases, the mixed layer shoals, and nitrate supply is reduced (Figure 1). If the BEUTI-derived “fall transition” is taken as the date at which cumulative BEUTI reaches 90% of its annual maximum, LUSI is greatly reduced, as is seen in 2008, 2012, 2016 and 2020 in the central and southern CCS (Figure S1). Thus, the biological utility of coastal upwelling, in terms of nitrate input to fuel primary production, typically declines through summer even as wind-driven upwelling continues.

The physical and biogeochemical phenology indices vary strongly depending on ENSO state with, for example, a later spring transition and lower TUMI during strong El Niño events (Figures 2 and 3). Cumulative CUTI and BEUTI derived for El Niño and La Niña composites differ in magnitude at all latitudes, driven largely by stronger alongshore winds (higher CUTI) in the La Niña years (Figure 3). However, differences in CUTI and BEUTI can also be driven by anomalous alongshore advection and propagation of coastal trapped waves associated with ENSO dynamics, as these processes affect water column structure independent of local wind forcing (Jacox et al., 2016). For example, the southern CCS had substantially reduced nitrate availability during the strong 1998 El Niño event relative to the nutrient-rich conditions during the 1999 La Niña event (Bograd & Lynn, 2001). In turn, variability in the timing of the biological upwelling season translates to decisions in top predator foraging ecology. For example, years with an earlier STI, longer upwelling season, and greater BEUTI-based TUMI resulted in a delayed departure of blue whales from the California Current foraging habitat (Oestreich et al., 2022). In general, the California Current ecosystem is less productive during El Niño phases (Chavez, et al., 2002 and references therein), consistent with the reduced nitrate flux shown here.

Earth system models project regional differences in the effects of climate change on coastal upwelling in the CCS (Bakun et al., 2015; Bograd et al., 2023; Rykaczewski et al., 2015). A projected poleward displacement of

et al., 2023; Pozo Buil et al., 2021). Further climate modeling studies are needed to clarify how changes in upwelling intensity, water column structure and nutrient supply, and their seasonal variations, will impact marine ecosystem productivity and function.

Data Availability Statement

Updated, downloadable versions of CUTI and BEUTI are made available by the Environmental Research Division of the NOAA Southwest Fisheries Science Center: <https://oceanview.pfeg.noaa.gov/products/upwelling/cutibeuti> (Environmental Research Division, 2024). The phenological upwelling indices used in this study (STI, LUSI, TUMI) were defined by Bograd et al. (2009): <https://agupubs.onlinelibrary.wiley.com/doi/pdf/10.1029/2008GL035933>.

References

- Asch, R. G. (2015). Climate change and decadal shifts in the phenology of larval fishes in the California Current ecosystem. *Proceedings of the National Academy of Sciences*, 112(30), E4065–E4074. <https://doi.org/10.1073/pnas.1421946112>
- Bakun, A. (1973). *Coastal upwelling indices, west coast of north America, 1946-71*. US Department of Commerce, National Oceanic and Atmospheric Administration, National Marine Fisheries Service.
- Bakun, A. (1975). *Daily and weekly upwelling indices, west coast of North America, 1967-73* (Vol. 693). Department of Commerce, National Oceanic and Atmospheric Administration, National Marine Fisheries Service.
- Bakun, A., Black, B. A., Bograd, S. J., García-Reyes, M., Miller, A. J., Rykaczewski, R. R., & Sydeman, W. J. (2015). Anticipated effects of climate change on coastal upwelling ecosystems. *Current Climate Change Reports*, 1(2), 85–93. <https://doi.org/10.1007/s40641-015-0008-4>
- Bograd, S. J., Jacox, M. G., Hazen, E. L., Lovecchio, E., Montes, I., Pozo, B. M., et al. (2023). Climate change impacts on eastern boundary upwelling systems. *Annual Review of Marine Science*, 15(1), 303–328. <https://doi.org/10.1146/annurev-marine-032122-021945>
- Bograd, S. J., & Lynn, R. J. (2001). Physical-biological coupling in the California current during the 1997-99 El Niño-La Niña cycle. *Geophysical Research Letters*, 28(2), 275–278. <https://doi.org/10.1029/2000gl012047>
- Bograd, S. J., Schroeder, I. D., Sarkar, N., Qiu, X., Sydeman, W. J., & Schwing, F. B. (2009). The phenology of coastal upwelling in the California Current. *Geophysical Research Letters*, 36(1), L01602. [Description of phenological indices: STI, LUSI, and TUMI]. <https://doi.org/10.1029/2008gl035933>
- Botsford, L. W., Lawrence, C. A., Dever, E. P., Hastings, A., & Largier, J. (2006). Effects of variable winds on biological productivity on continental shelves in coastal upwelling systems. *Deep Sea Research Part II: Topical Studies in Oceanography*, 53(25–26), 3116–3140. <https://doi.org/10.1016/j.dsr2.2006.07.011>
- Chavez, F. P., Pennington, J. T., Castro, C. G., Ryan, J. P., Michiaski, R. P., Schilling, B., et al. (2002). Biological and chemical consequences of the 1997-1998 El Niño in central California waters. *Progress in Oceanography*, 54(1–4), 205–232. [https://doi.org/10.1016/s0079-6611\(02\)00050-2](https://doi.org/10.1016/s0079-6611(02)00050-2)
- Colas, F., Capet, X., McWilliams, J. C., & Shchepetkin, A. (2008). 1997–1998 El Niño off Peru: A numerical study. *Progress in Oceanography*, 79(2–4), 138–155. <https://doi.org/10.1016/j.pocean.2008.10.015>
- Cushing, D. H. (1990). Plankton production and year-class strength in fish populations: An update of the match/mismatch hypothesis. *Advances in Marine Biology*, 26, 249–293.
- Durant, J. M., Hjermmann, D. Ø., Ottersen, G., & Stenseth, N. C. (2007). Climate and the match or mismatch between predator requirements and resource availability. *Climate Research*, 33(3), 271–283. <https://doi.org/10.3354/cr033271>
- Environmental Research Division. (2024). Upwelling indices. Retrieved from <https://oceanview.pfeg.noaa.gov/products/upwelling/cutibeuti>
- Frischknecht, M., Munnich, M., & Gruber, N. (2015). Remote versus local influence of ENSO on the California Current System. *Journal of Environmental Research*, 120(2), 1353–1374. <https://doi.org/10.1002/2014jc010531>
- García-Reyes, M., Largier, J. L., & Sydeman, W. J. (2014). Synoptic-scale upwelling indices and predictions of phyto-and zooplankton populations. *Progress in Oceanography*, 120, 177–188. <https://doi.org/10.1016/j.pocean.2013.08.004>
- Jacox, M. G., Bograd, S. J., Hazen, E. L., & Fiechter, J. (2015). Sensitivity of the California Current nutrient supply to wind, heat, and remote ocean forcing. *Geophysical Research Letters*, 42(14), 5950–5957. <https://doi.org/10.1002/2015gl065147>
- Jacox, M. G., Edwards, C. A., Hazen, E. L., & Bograd, S. J. (2018). Coastal upwelling revisited: Ekman, Bakun, and improved upwelling indices for the U.S. West Coast. *Journal of Geophysical Research: Oceans*, 123(10), 7332–7350. <https://doi.org/10.1029/2018jc014187>
- Jacox, M. G., Hazen, E. L., & Bograd, S. J. (2016). Optimal environmental conditions and anomalous ecosystem responses: Constraining bottom-up controls of phytoplankton biomass in the California Current System. *Scientific Reports*, 6(1), 27612. <https://doi.org/10.1038/srep27612>
- Kara, A. B., Rochford, P. A., & Hurlburt, H. E. (2000). An optimum definition for ocean mixed layer depth. *Journal of Geophysical Research*, 105(C7), 16803–16821. <https://doi.org/10.1029/2000jc900072>
- Lamont, T., García-Reyes, M., Bograd, S. J., Van Der Linden, C. D., & Sydeman, W. J. (2018). Upwelling indices for comparative ecosystem studies: Variability in the Benguela upwelling system. *Journal of Marine Systems*, 188, 3–16. <https://doi.org/10.1016/j.jmarsys.2017.05.007>
- Marchesiello, P., & Estrade, P. (2010). Upwelling limitation by onshore geostrophic flow. *Journal of Marine Research*, 68(1), 37–62. <https://doi.org/10.1357/002224010793079004>
- Neveu, E., Moore, A. M., Edwards, C. A., Fiechter, J., Drake, P., Crawford, W. J., et al. (2016). An historical analysis of the California Current circulation using ROMS 4D-Var: System configuration and diagnostics. *Ocean Modelling*, 99, 133–151. <https://doi.org/10.1016/j.ocemod.2015.11.012>
- Oestreich, W. K., Abrahms, B., McKenna, M. F., Goldbogen, J. A., Crowder, L. B., & Ryan, J. P. (2022). Acoustic signature reveals blue whales tune life-history transitions to oceanographic conditions. *Functional Ecology*, 36(4), 882–895. <https://doi.org/10.1111/1365-2435.14013>
- Pozo Buil, M., Jacox, M. J., Fiechter, J., Alexander, M. A., Bograd, S. J., Curchitser, E. N., et al. (2021). Dynamically downscaled ensemble projections for the California Current System. *Frontiers in Marine Science*, 8, 612874. <https://doi.org/10.3389/fmars.2021.612874>
- Rykaczewski, R. R., Dunne, J. P., Sydeman, W. J., García-Reyes, M., Black, B. A., & Bograd, S. J. (2015). Poleward displacement of coastal upwelling-favorable winds in the ocean's eastern boundary currents through the 21st century. *Geophysical Research Letters*, 42(15), 6424–6431. <https://doi.org/10.1002/2015gl064694>
- Schwing, F. B., O'Farrell, M., Steger, J. M., & Baltz, K. (1996). Coastal upwelling indices, west coast of North America. NOAA Tech. Rep., NMFS, SWFSC, 231, 144.